Experimental study of liquid to air membrane energy exchanger (LAMEE) performance by measuring its temperature fields

Junze Chu, Ziwei Chen, Hongyu Bai, Jie Zhu*

Department of Architecture and Built Environment, the University of Nottingham

University Park, Nottingham, NG7 2RD, UK

*Corresponding author, E-mail address: jie.zhu@nottingham.ac.uk

Abstract

Many studies have already been conducted to assess liquid to air membrane energy exchanger (LAMEE) performance by numerical and experimental methods. However, the LAMEE temperature field is still an unknown area due to the operation difficult. In this study, an experimental method is adopted to investigate the performance of LAMEE by measuring its temperature fields. The effects of main parameters such as the solution temperature, solution concentration and air relative humidity, are investigated. The results show that the air relative humidity and solution temperature have negative influences on the LAMEE efficiency. It is found that the total effectiveness reduces 2.7% and 7.7% when the air relative humidity increases from 62% to 74%, and the solution temperature changes from 18℃ to 26℃, respectively. Increasing the solution concentration decreases the sensible effectiveness while enhancing the latent and total effectiveness. The total effectiveness increases 3.5% as the solution concentration increase from 30% by 39%. These results are useful to optimize the LAMEE in the future.

Key words: Experimental method; parameter effects; LAMEE performance, temperature field.

1. Introduction

Energy crisis becomes a serious problem in recent years and buildings consume about forty percent of the total energy [1]. Heating, cooling and ventilation take large proportion in the building energy consumption, and people spend most of their time on indoor activities [2]. Liquid desiccant air conditioning (LDAC) system saves large amount of energy compared with the traditional mechanical type in dealing with latent heat; low regeneration temperature means that LDAC system can be powered by low grade thermal energy such as waste heat or

renewable energy, which shows the potential of its application in the rural areas and developing countries [3]. Carryover problem of LDAC can be avoided by applying semi-permeable membranes in dehumidifier and regenerator [4]. The semi-permeable membranes separate the air stream and desiccant solution to prevent the carryover of liquid desiccant droplets. In a liquid to air membrane energy exchanger (LAMEE), only water vapour and heat can pass through the membrane, while the solution is not allowed to go through the membrane. Although the membrane increases the moisture and heat transfer resistances in the LDAC, it provides a safety environment for human beings. There are a lot of numerical study for the LAMEE temperature field [5-10], however the experimental test of the temperature field is still not carried out. In this paper an experimental method is adopted to investigate the performance of a LAMEE by measuring its temperature fields. The experimental results of the LAMEE temperature fields can be applied for validating the numerical modelling; moreover, it could be used as the reference data for optimization of the LAMEE, for example, adjusting the solution distribution according to the temperature field (more solution at high temperature area).

Nomenclature	
C	Concentration (kg/m^3)
c_p	Specific heat capacity (J/kgK)
Cr*	Heat capacity ratio
d	Width of the channel (m)
D	Diffusivity (m^2/s)
H	Height of the LAMEE (m)
H*	Operating factor
k	Thermal conductivity (W/mK)
k_m	Membrane water vapour permeability (kg/m s)
L	Length of the LAMEE (m)
LAMEE	Liquid to air membrane energy exchanger

|	
LDAC	Liquid desiccant air conditioning
RH	Relative humidity (%)
T	Temperature (℃)
W	Width of the LAMEE (m)
$W_{air/sol}$	Humidity ratio (kg/kg)
Greek symbols	
ε	Effectiveness
δ	Membrane thickness (m)
ρ	Density (kg/m^3)
Subscripts	
air	Air flow
in	Inlet
lat	Latent
mem	Membrane
out	Outlet
sen	Sensible
sol	Solution flow
tot	Total

45

2. Methodology

47 In order to get the temperature field inside the membrane based flat plate dehumidifier, a
48 number of temperature sensors are installed in one air channel and one adjacent solution
49 channel, the dehumidifier structure and geometry information are shown in Fig.1. Each channel
50 is installed with 15 sensors as indicated in Fig.2. In the air channel, every 5 sensors are stuck
51 in one strip in horizontal direction, while in the solution channel, every 3 sensors are fixed in
52 one strip in vertical direction.

53
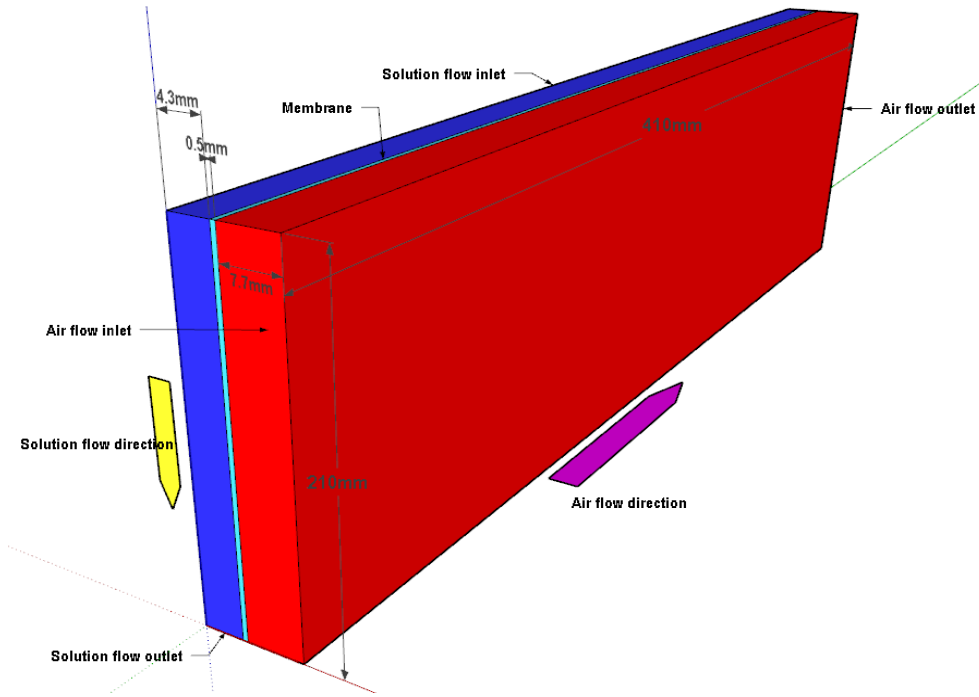
Fig.1: Structure and geometry information for the air and solution channels.

| (a) | (b) |
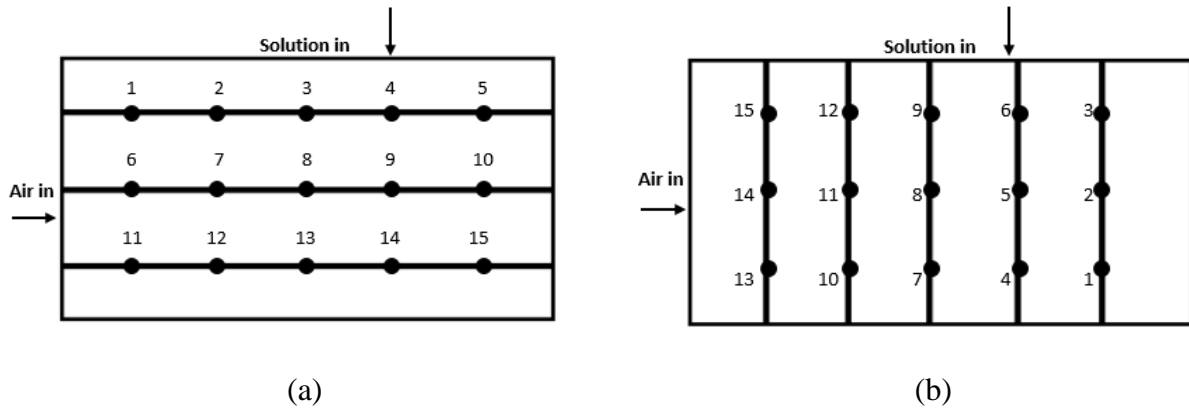
Fig.2: Sensor arrangements in (a) air channel; (b) solution channel.

The specifications of the dehumidifier and membrane, and the desiccant solution and air properties are listed in Table1.

Table 1: Dehumidifier specifications, membrane physical properties, air and desiccant solution properties.

Symbol	Unit	Value	Symbol	Unit	Value
L	m	0.41	k_{air}	W/mK	0.03
W	m	0.23	k_{sol}	W/mK	0.53
H	m	0.21	D_{air}	m^2/s	2.46×10^{-5}

4

d_{air}	m	0.0077		D_{sol}	m^2/s	0.892×10^{-2}
d_{sol}	m	0.0043		$c_{p,air}$	J/kgK	1020
δ_{mem}	m	0.5×10^{-3}		$c_{p,sol}$	J/kgK	3200
k_{mem}	W/mK	0.3		ρ_{air}	kg/m^3	1.29
$k_{m,mem}$	Kg/ms	3.87×10^{-6}		ρ_{sol}	kg/m^3	1247

3. Performance index

Effectiveness is the commonly used performance index in energy exchanger. Sensible, latent and total effectiveness are applied to investigate the energy exchanger performance respectively. The sensible effectiveness is the ratio between the actual and maximum possible sensible heat transfer rates in the energy exchanger and given by:

$$\varepsilon_{sen} = \frac{T_{air,in} - T_{air,out}}{T_{air,in} - T_{sol,in}} \tag{1}$$

Where ε_{sen} is the sensible effectiveness, $T_{air,in}$ is the inlet air temperature (℃), $T_{air,out}$ is the outlet air temperature (℃), $T_{sol,in}$ is the inlet solution temperature (℃).

The latent effectiveness is the ratio between actual and maximum possible latent heat transfer rates in the energy exchanger and defined as:

$$\varepsilon_{lat} = \frac{W_{air,in} - W_{air,out}}{W_{air,in} - W_{sol,in}} \tag{2}$$

Where ε_{lat} is the latent effectiveness, $w_{air,in}$ is the inlet air humidity ratio (kg/kg), $w_{air,out}$ is the outlet air humidity ratio (kg/kg), $w_{sol,in}$ is the inlet solution equilibrium specific humidity ratio (kg/kg).

The total effectiveness is the ratio between the actual and maximum possible energy transfer rates in the energy exchanger and given by:

$$\varepsilon_{tot} = \frac{\varepsilon_{sen} + H^* \varepsilon_{lat}}{1 + H^*} \tag{3}$$

Where ε_{tot} is the total effectiveness, H^* is the operating factor.

Equations (1) to (3) are only meaningful when the solution capacity rate is higher than or equal to the air capacity rate ($Cr^* \geq 1$).

4. Experiment setting

The basic experimental parameters are set as: 20℃ inlet lithium chloride solution with 33% concentration; 30℃ inlet air temperature with 70% relative humidity.The more detail settings are shown in Table 2.

Table 2 : Experiment settings.

Num	Air RH (%)	Num	T sol (℃) C_{sol}=30%	Num	T sol (℃) C_{sol}=33%	Num	T sol (℃) C_{sol}=36%	Num	T sol (℃) C_{sol}=39%
1	62	5	18	10	18	15	18	20	18
2	66	6	20	11	20	16	20	21	20
3	70	7	22	12	22	17	22	22	22
4	74	8	24	13	24	18	24	23	24
		9	26	14	26	19	26	24	26

30%, 33%, 36% and 39% concentration solutions are tested under five different inlet solution temperatures.

5. Results & discussion

The temperature field results for basic parameter setting are shown in Table 3. From Table 3, it can be seen that the air temperature decreases along its flow direction and increases in the vertical direction. As for the solution temperature, it increases along the solution flow direction, the highest temperature occurs at the left bottom corner. The temperature maps are plotted with linear interpolation method as shown in Fig.3.

Table 3: Temperature field results for basic parameter setting.

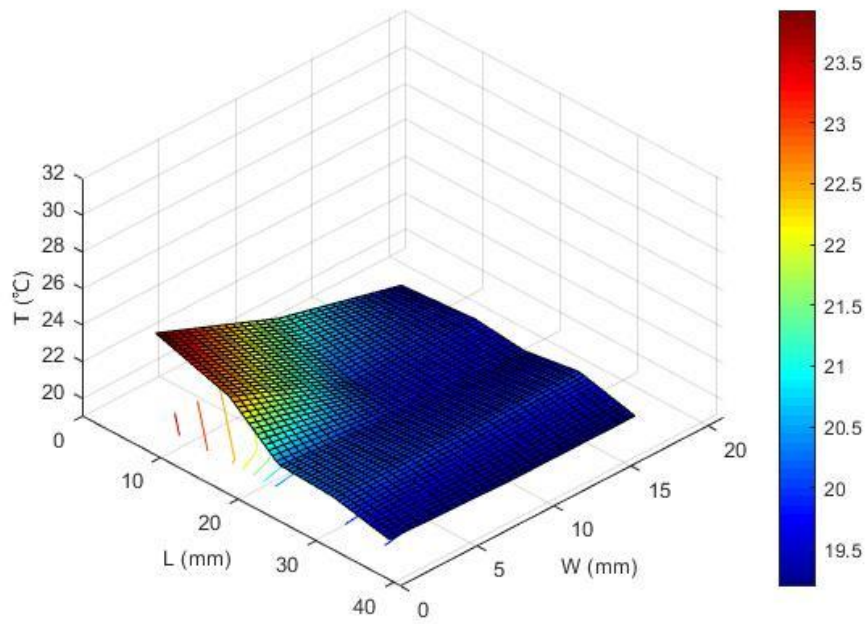| Air side (℃)						Solution side (℃)				
1	2	3	4	5		15	12	9	6	3
30.146	30.053	29.696	27.939	26.531		19.515	19.822	19.52	19.975	19.157
6	7	8	9	10		14	11	8	5	2
30.428	30.069	29.901	28.061	27.161		21.229	19.954	19.783	19.975	19.179
11	12	13	14	15		13	10	7	4	1
32.232	31.863	30.445	28.384	27.553		23.937	22.608	20.33	20.155	19.415
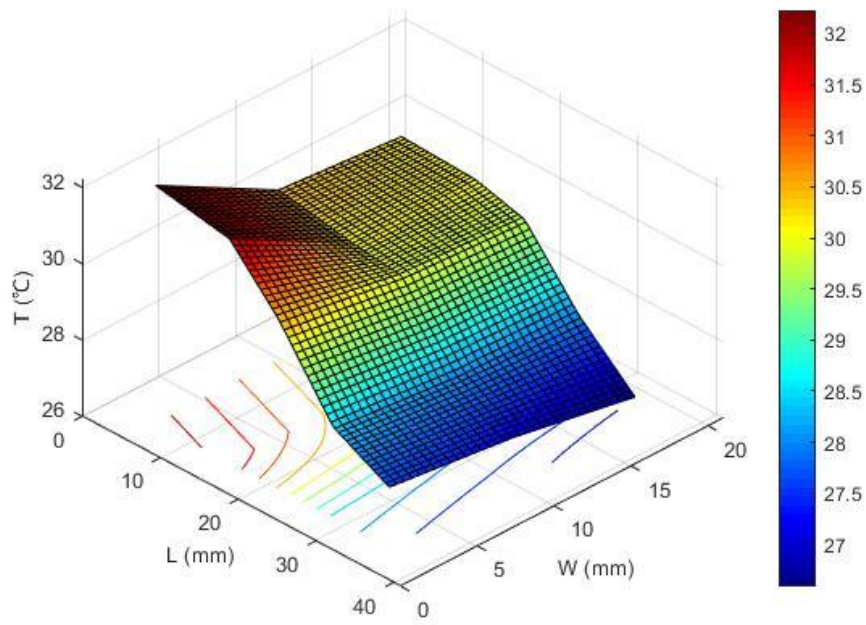
105

106   (a)
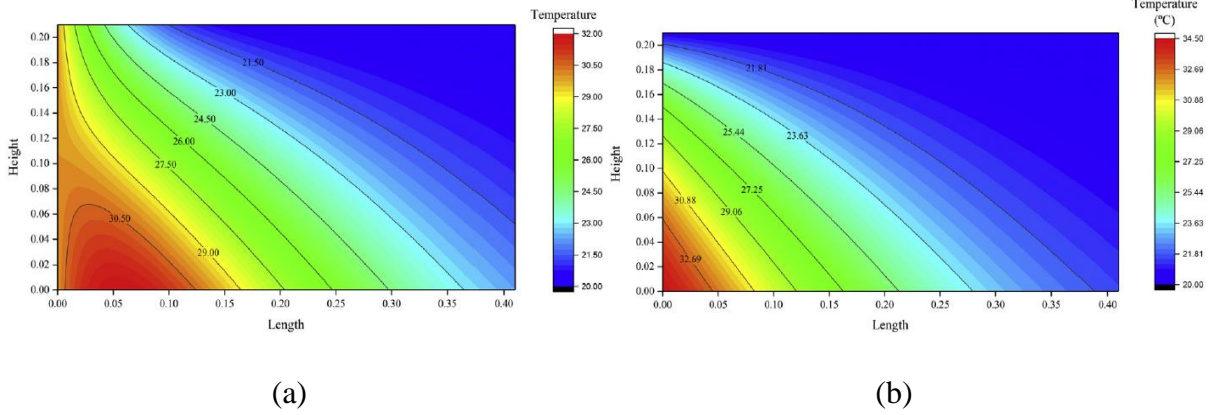
107

108   (b)

109   Fig.3: (a) Air temperature field; (b) Solution temperature field.

7

Fig.4: Temperature fields in previous work: (a) air side; (b) solution side [11].

From Fig.3 (a), it can be seen that the highest air temperature area is located at the cross section of the air inlet and solution outlet. The air temperature in that area is even higher than the inlet air temperature because the plenty of latent heat is released. As indicated in Fig.3 (b), the highest solution temperature area is located at the bottom-left corner while the lowest temperature field is at the top-right corner. Compared with the previous simulation results shown in Fig.4, the experimental air and solution temperature variation tendencies correspond with the simulated ones. The similar variation tendency can be found in literature [9]. Therefore, the experimental results are convincible and can be used to investigate the LAMEE performance.
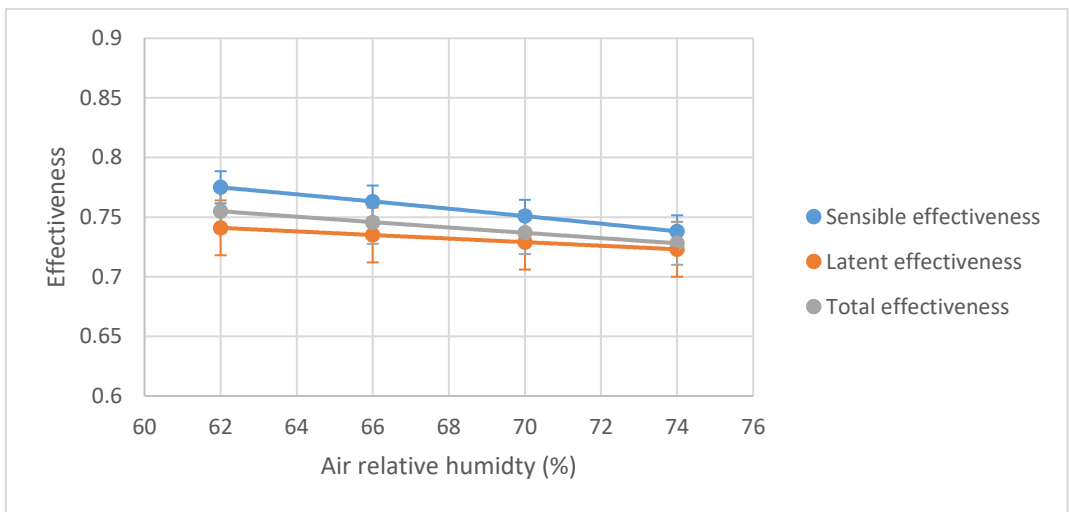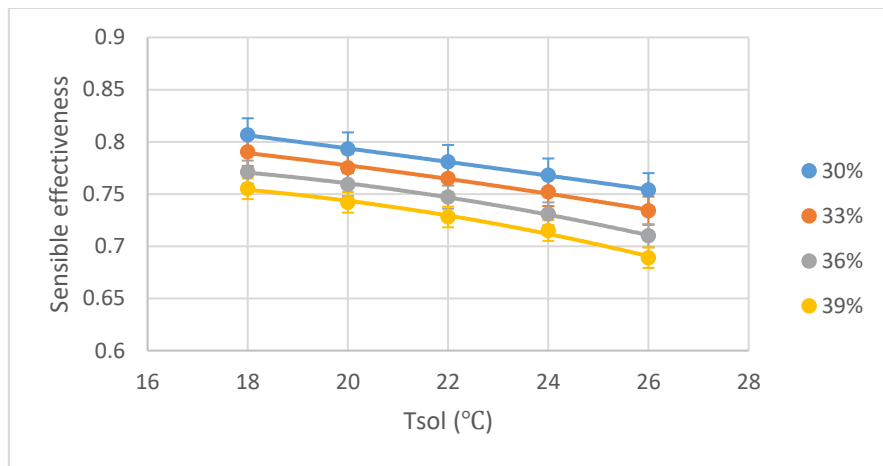

Fig. 5: Sensible, latent and total effectiveness variations with air RH.

Fig.5 presents the air relative humidity influences on the sensible, latent and total effectiveness of the LAMEE. Generally speaking, the air RH has little negative influence on the LAMEE performance. For example, the sensible effectiveness decreases from 0.775 to 0.738 when the air RH increases from 62% to 76%. The main reason for this case is more latent heat released in the solution side. In the tested range, the latent effectiveness decreases only about 0.018 but the moisture remove rate increases 27.38%. Therefore the performance index should be properly adopted in practical application. The total effectiveness also decreases a little with the air RH about 0.027 in the tested range.

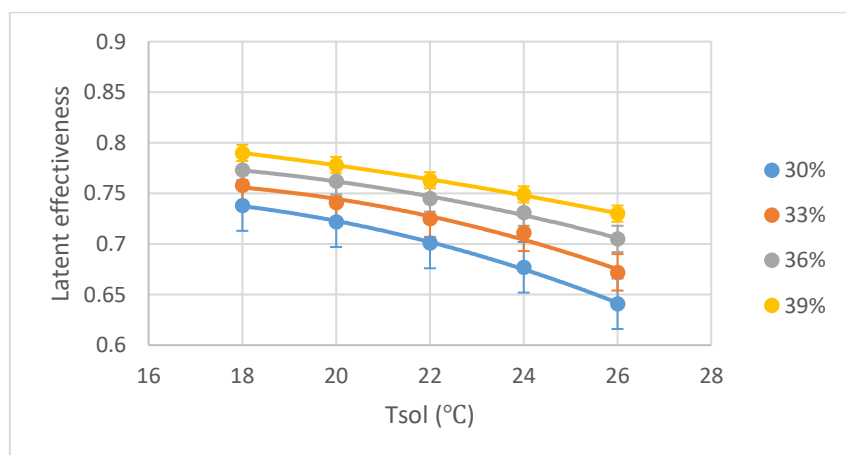Fig.6: Sensible effectiveness variations with T_{SOL} under different C_{SOL}.
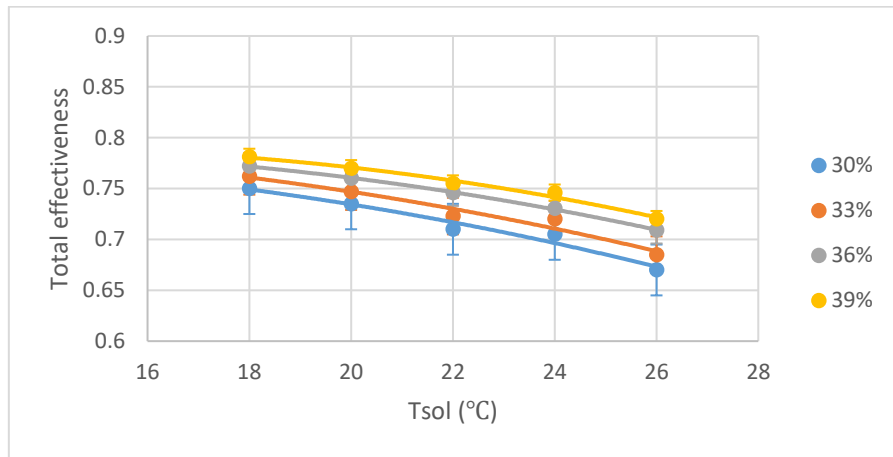
141   Fig.7: Latent effectiveness variations with T_{SOL} under different C_{SOL}.

142

143

144

145   Fig.8: Total effectiveness variations with T_{SOL} under different C_{SOL}.

146   Figs.6, 7 and 8 indicate the solution temperature and concentration influences on the

147   effectiveness. It is obvious that the solution temperature has negative influence on the sensible,

148   latent and total effectiveness. Increasing the solution temperature decreases the vapour pressure

149   difference between the air and desiccant solution sides, then reduces the dehumidification

150   performance. Enhancing the solution temperature reduces both the denomination and

151   numerator in Eq. (1) at the same time but with larger numerator reduction. The influence of the

152   liquid desiccant solution temperature on LAMEE performance is more obvious than the air

153   RH's. For example, at C_{SOL}=33%, the total effectiveness reduces from 0.762 to 0.685 when the

154   solution temperature changes from 18°C to 26 °C; while at C_{SOL}= 39%, the corresponding total

155   effectiveness decreases from 0.781 to 0.720.

156   As for the solution concentration effect, increasing the solution concentration decreases the

157   sensible effectiveness due to more moisture absorbed. In opposite, the high concentration

158   solution makes contribution to the latent and total effectiveness. However, the influence on the

159   total effectiveness is insignificant. For instance, the total effectiveness decreases from 0.770 to

160   0.735 when the solution concentration changes from 39% to 30% at the inlet solution

161   temperature of 20 °C. Therefore for the practical application, this should be considered because

162   only 5 percent or less effectiveness improvement is achieved in the experimental test.

163   **6. Conclusion**

164　In this paper, the temperature field of a cross flow LAMEE is investigated experimentally.

165　Some conclusions can be drawn as follows:

166

167　　• The experimental temperature fields have the correct variation tendency and can be
168　　　used to optimise the LAMEE performance.

169　　• Air relative humidity has little effect on the LAMEE performance. In the tested range,
170　　　the sensible, latent and total effectiveness only decrease 0.037, 0.018 and 0.027
171　　　respectively.

172　　• Desiccant solution temperature has obviously negative influences on the sensible, latent
173　　　and total effectiveness. At C_{SOL}=33%, the total effectiveness reduces from 0.762 to
174　　　0.685 when the solution temperature changes from 18 ℃ to 26 ℃; at C_{SOL}= 39%, the
175　　　corresponding total effectiveness decreases from 0.781 to 0.720.

176　　• The solution concentration has the negative effect on the sensible effectiveness while it
177　　　has the positive influences on the latent and total effectiveness. However, only less than
178　　　5% effectiveness improvement is achieved in the experimental test. Therefore, its
179　　　limited effect should be considered in practical application.

180

181　**Conflict of interest**

182　The authors declared that there is no conflict of interest.

183　**References**

184　[1] A.M Omer. Energy, environment and sustainable development. Renewable and Sustainable
185　　　Energy Reviews 2008; 12:2265–300.

186　[2] X.D Cao, X.L Dai, J.J Liu. Building energy-consumption status worldwide and the state-
187　　　of-the-art technologies for zero-energy buildings during the past decade. Energy and
188　　　Buildings 2016; 128: 198–213.

189　[3] K.Daou, R.Z Wang, Z.Z. Xia. Desiccant cooling air conditioning: a review. Renewable and
190　　　Sustainable Energy Reviews 2006; 10: 55-77.

191　[4] A.H Abdel-Salam, G.M Ge, G.J Simonson. Performance analysis of a membrane liquid
192　　　desiccant air-conditioning system. Energy and Buildings 2013; 62:559–569.

193　[5] Y.M Luo, HX Yang, L Lu, RH Qi. A review of the mathematical models for predicting the
194　　　heat and mass transfer process in the liquid desiccant dehumidifier. Renewable and
195　　　Sustainable Energy Reviews 2014; 31:587-599.

196 [6] Y.M Luo, HX Yang, Y Chen, YH Wang. Application of CFD Model in Analyzing the
197   Performance of a Liquid Desiccant Dehumidifier. Energy Procedia 2016; 88:491-497.
198 [7] X.H Liu, Y Jiang, K.Y Qu. Heat and mass transfer model of cross flow liquid desiccant
199   air dehumidifier/regenerator. Energy Conversion and Management 2007; 48:546-554.
200 [8] S.A Nada. Air cooling-dehumidification/desiccant regeneration processes by a falling
201   liquid desiccant film on finned-tubes for different flow arrangements. International Journal
202   of Thermal Sciences 2017; 113:10-19.
203 [9] R.S Das, S J. Performance characteristics of cross-flow membrane contactors for liquid
204   desiccant systems. Applied Energy 2015; 141: 1-11.
205 [10] S.M Huang, M.L Yang, X.X Yang. Performance analysis of a quasi-counter flow parallel-
206   plate membrane contactor used for liquid desiccant air dehumidification. Applied Thermal
207   Engineering 2014; 63:323-332.
208 [11] H.Y Bai, J Zhu, Z.W Chen, J.Z Chu. Parametric analysis of a cross-flow membrane-based
209   parallel-plate liquid desiccant dehumidification system: Numerical and experimental data.
210   Energy and Buildings 2018; 158:494-508.